Water Research xxx (2018) xxx-xxx

Contents lists available at ScienceDirect

Water Research

journal homepage: www.elsevier.com

# Seasonal pattern of anthropogenic salinization in temperate forested headwater streams

Anthony J. Timpano[a, *], Carl E. Zipper[b], David J. Soucek[c], Stephen H. Schoenholtz[a]

[a] Virginia Water Resources Research Center, Virginia Tech, 310 West Campus Dr, RM 210, Blacksburg, VA 24061, USA
[b] Crop and Soil Environmental Sciences, Virginia Tech, 185 Ag Quad Ln, RM 416, Blacksburg VA 24061, USA
[c] Illinois Natural History Survey, 1816 S. Oak St, Champaign IL 61820, USA

ARTICLE INFO

*Article history:*
Received 13 October 2017
Received in revised form 29 December 2017
Accepted 4 January 2018
Available online xxx

*Keywords:*
Freshwater salinization
Major ions
Conductivity
Coal mining
Periodic functions
Seasonality

ABSTRACT

Salinization of freshwaters by human activities is of growing concern globally. Consequences of salt pollution include adverse effects to aquatic biodiversity, ecosystem function, human health, and ecosystem services. In headwater streams of the temperate forests of eastern USA, elevated specific conductance (SC), a surrogate measurement for the major dissolved ions composing salinity, has been linked to decreased diversity of aquatic insects. However, such linkages have typically been based on limited numbers of SC measurements that do not quantify intra-annual variation. Effective management of salinization requires tools to accurately monitor and predict salinity while accounting for temporal variability. Toward that end, high-frequency SC data were collected within the central Appalachian coalfield over 4 years at 25 forested headwater streams spanning a gradient of salinity. A sinusoidal periodic function was used to model the annual cycle of SC, averaged across years and streams. The resultant model revealed that, on average, salinity deviated approximately ±20% from annual mean levels across all years and streams, with minimum SC occurring in late winter and peak SC occurring in late summer. The pattern was evident in headwater streams influenced by surface coal mining, unmined headwater reference streams with low salinity, and larger-order salinized rivers draining the study area. The pattern was strongly responsive to varying seasonal dilution as driven by catchment evapotranspiration, an effect that was amplified slightly in unmined catchments with greater relative forest cover. Evaluation of alternative sampling intervals indicated that discrete sampling can approximate the model performance afforded by high-frequency data but model error increases rapidly as discrete sampling intervals exceed 30 days. This study demonstrates that intra-annual variation of salinity in temperate forested headwater streams of Appalachia USA follows a natural seasonal pattern, driven by interactive influences on water quantity and quality of climate, geology, and terrestrial vegetation. Because climatic and vegetation dynamics vary annually in a seasonal, cyclic manner, a periodic function can be used to fit a sinusoidal model to the salinity pattern. The model framework used here is broadly applicable in systems with streamflow-dependent chronic salinity stress.



## 1. Introduction

Freshwater is increasingly at risk globally from anthropogenic salinization (Millennium Ecosystem Assessment, 2005; Cañedo-Argüelles et al., 2013), which is the increased concentration of dissolved major ions (i.e., $Ca^{2+}$, $Mg^{2+}$, $Na^{+}$, $K^{+}$, $Cl^{-}$, $SO_4^{2-}$, $HCO_3^{-}$) above natural background levels (Williams, 1987, 2001). Salinization can cause adverse effects to aquatic biodiversity, ecosystem function, human health, and ecosystem services, which is why development of policies and tools for management of salinity is an urgent need (Cañedo-Argüelles et al., 2016). Factors causing salinization include agricultural irrigation, water abstraction, road de-icing, urban runoff, and, in many world regions, mining (Schreck, 1995; Goetsch and Palmer, 1997; Hancock et al., 2005; Pond et al., 2008; Cañedo-Argüelles et al., 2013).

In headwater streams of the temperate eastern deciduous forests in USA, salinity is identified as a biotic stressor and threat to aquatic insect diversity where naturally-dilute streams (Griffith, 2014) are affected by major ions released from geologic materials that have been disturbed by mining (Griffith et al., 2012; Cormier and Suter, 2013). Coal surface mining disturbs geologic materials that occur naturally deep below the land surface, exposing minerals to ambient environmental conditions and causing accelerated weathering. Environmental waters solubilize weathering reaction products, primarily mineral-origin salts (Daniels et al., 2016), often causing salinity of mine-water discharges to be elevated relative to the region's natural waters (Pond et al., 2008, 2014; Griffith et al., 2012; Evans et al., 2014; Timpano et al., 2015). Elevated specific conductance (SC), a surrogate measurement for the major dissolved ions composing salinity, has been linked to decreased richness and evenness of aquatic insect communities (Pond et al., 2008), with generally sensitive taxa from the orders Ephemeroptera, Plecoptera, and Trichoptera most strongly affected (Pond, 2010, 2012; Timpano et al., 2015). However, such linkages have been based on SC measured infrequently, even as

* Corresponding author.
*Email address:* atimpano@vt.edu (A.J. Timpano)

https://doi.org/10.1016/j.watres.2018.01.012
0043-1354/

rarely as with a single measurement per study stream (Bernhardt et al., 2012). Discrete, one-time measurements of SC may not be sufficient to quantify accurately the intra-annual variation affecting organismal life-cycle exposure.

It has long been recognized that surface-water solutes are influenced strongly by geology, hydrology, precipitation, and evapotranspiration (ET) (Gibbs, 1970), as well as the interaction of climate and geology with terrestrial flora and soils (Hem, 1985). It has also been observed that in temperate streams with forested catchments, surface water solutes often exhibit strong seasonal variability (e.g., Likens and Bormann, 1995), which is driven largely by land use and rates of precipitation and ET (Helsel and Hirsch, 2002). Therefore, it is reasonable to expect salinity to vary seasonally as a function of one or more of these factors. If precipitation and geologic influence in headwater streams in the study region are relatively constant, stream water yield, and therefore stream salinity, should be influenced by ET and therefore exhibit a cyclic annual pattern roughly concurrent with the water cycle. Further, because ET is a natural influence on streamflow, we expect salinity patterns to be similar in both reference and test streams with partially forested catchments, despite the anthropogenic alterations of geology and weathering rates resultant from coal mining in the latter.

Our first objective was to model the annual pattern of salinity, as measured by SC in freshwater streams of Appalachia USA, using a periodic function to characterize the cyclic nature of the pattern. Recognizing the practical hurdles to obtaining high-frequency SC data, our second objective was to evaluate the effectiveness of alternative sampling intervals for describing the SC pattern. Where salinity does vary in a regular seasonal way, characterization of the annual pattern could enhance capability to quantify salt exposures to biota as well as to mitigate salinization effects.

## 2. Methods

### *2.1. Stream selection*

We selected headwater streams within the U. S. Environmental Protection Agency (USEPA) Level IV Central Appalachian ecoregion 69d (Omernik and Griffith, 2014) of Virginia and West Virginia with varied degrees of salinization by surface coal mining. This region was an ideal study system because coal mining land use in the region is a common, reliable source of salinization and the headwater stream segments allowed us to model salinity patterns free from excessive confounding influences. We visited more than 260 streams to select 25 streams (Fig. 1) that spanned a gradient of SC, yet were comparable to un-mined reference streams with respect to riparian and instream habitat quality. Sample reaches were designated first-order per the USEPA National Hydrography Dataset Plus (USEPA, 2012) and had mean catchment area (±SD) of 331 ± 226 ha. Five streams free of salinization from mining and representing best available habitat and water quality in the region were considered "reference" streams (mean SC range: 24–130 µS/cm), and 20 "test" streams spanned a gradient of salinity (mean SC range: 220–1438 µS/cm) while maintaining reference-quality habitat. See Timpano et al. (2015) for further detail of stream selection methods. The source of saline leachate for test streams was weathering of mine spoil, which was either consolidated in stream channels in what are known as "valley fills" or left unconsolidated on the hillslope after contour mining.

Forest coverage in each catchment was estimated in a GIS by first delineating watersheds upstream of the sample reach. Then proportions of forest land cover were calculated by geospatial analysis of existing databases (Li et al., 2015; MRLC, 2017), followed by analysis of available high-resolution aerial imagery for assessment of re-

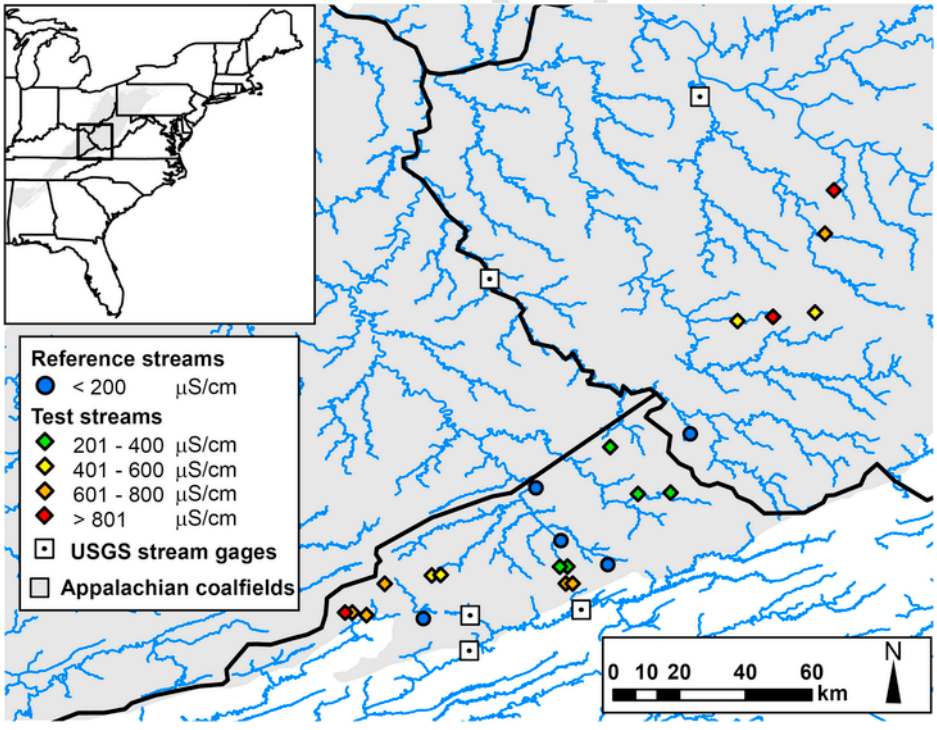


**Fig. 1.** Map of study streams in the central Appalachian coalfield of eastern USA. Study stream markers are colored by mean specific conductance. Data from stream gages maintained by U.S. Geological Survey (USGS) were used for evaluating model performance with larger-order rivers.

cent forest-cover changes resulting from subsequent mining that occurred during the study period in a small number of test-stream watersheds.

### 2.2. Regional climate and streamflow

The central Appalachian ecoregion is characterized by mixed mesophytic forest (Omernik, 1987) with temperate climate and relatively uniform precipitation throughout the year (Baily, 1995). Precipitation and temperature for the study region were estimated using data from four weather stations that span the extent of study stream locations (USNOAA, 2017). The 30-year mean annual precipitation for those stations was 1179 mm and the mean monthly temperature ranged from 0.6 °C to 22.8 °C. Precipitation averaged 1227 mm per year for the period 2011–2015, with mean monthly precipitation ranging from 70 mm in November to 152 mm in July (Fig. 2). Streamflow followed a seasonal pattern in the study region during 2011–2015, with highest flows in winter and spring and lowest flows in summer and fall (Fig. 3). Mean monthly SC (±SE) of precipitation at three gauges in the region during 2011–2015 was 8.3 ± 0.28 µS/cm, was not significantly different among months for any gauge (ANOVA, $p > 0.05$), and did not follow a pattern matching precipitation or streamflow (data not shown; from National Atmospheric Deposition Program sites KY22, VA13, and WV04).

### 2.3. Data collection

Long-term, high-frequency measurement of SC and water temperature was achieved using automated dataloggers (HOBO Freshwater Conductivity Data Logger, model U24-001, Onset Computer Corp., Bourne, Massachusetts USA). Dataloggers were installed upon completion of stream selection (between July and October 2011), and continued recording measurements at 30-min intervals through October 2015. All dataloggers were installed within stream reaches that

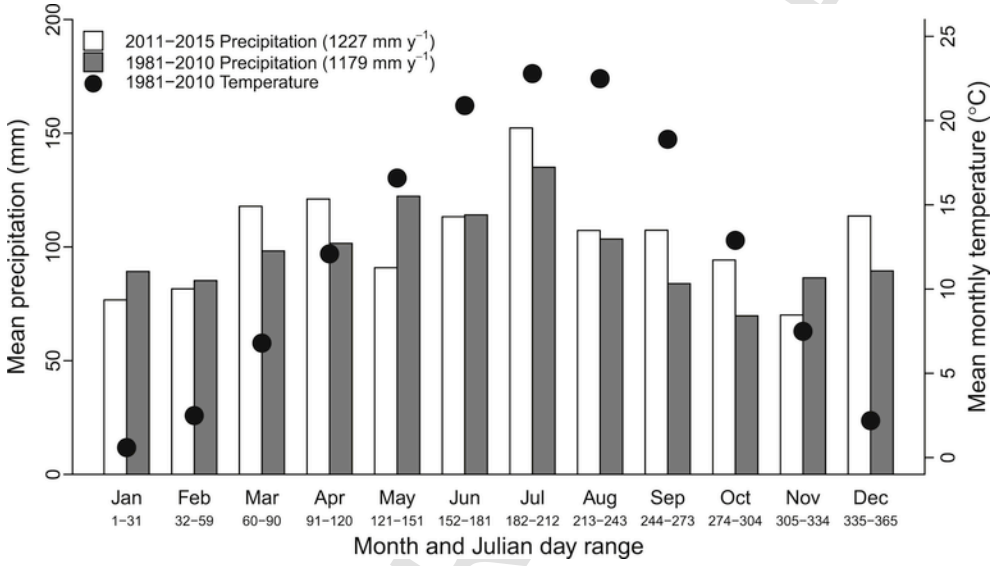


**Fig. 2.** Monthly mean precipitation and temperature. Data are from four U.S. National Weather Service stations in the study region: Wise 1 SE (station 449215) and Grundy (station 443640) in Virginia, and Oceana 2 SE (station 466600) and London Locks (station 465365) in West Virginia.

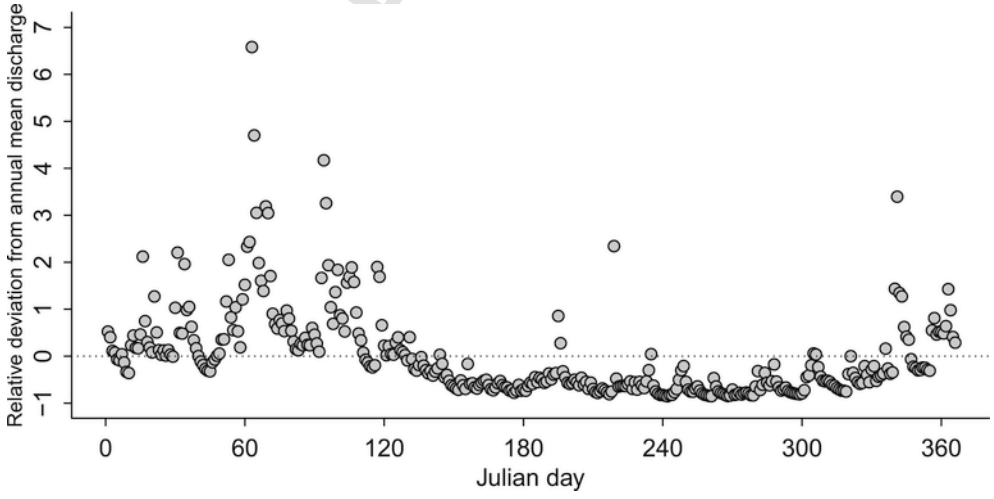


**Fig. 3.** Annual streamflow pattern typical of the region. Average of daily mean discharge values for 5 second- and third-order streams in the study region of southwestern Virginia, southern West Virginia, and eastern Kentucky during 2011–2015. Daily discharge data are presented as relative deviation from stream-wise annual mean daily discharge. Data are from U.S. Geological Survey gaging stations 03198350, 03206600, 03207965, 03210000, and 03213500.

were free from immediate upstream anthropogenic influence other than coal mining.

To assess ionic composition of stream water, grab-samples were collected approximately monthly at each stream during baseflow (i.e., flow not influenced by storm flow) from May 2011 through April 2013. Stream water samples were filtered immediately using polyvinylidene difluoride syringe filters with a pore size of 0.45 μm and stored in sterile polyethylene sample bags. Aliquots for analysis of cations were preserved to pH < 2 with 1 + 1 concentrated ultrapure nitric acid. All samples were transported to the laboratory on ice and stored at 4 °C until analysis.

In the laboratory, water samples were analyzed for major cations using an inductively coupled plasma-optical emission spectrometer (Varian Vista MPX ICP-OES w/ICP Expert software, Varian Instruments, Walnut Creek, California USA) to measure dissolved concentrations of $Ca^{2+}$, $Mg^{2+}$, $K^{+}$, and $Na^{+}$ (APHA, 2005). An ion chromatograph (Dionex DX500, Dionex Corp., Sunnyvale, California USA) was used to measure $Cl^{-}$ and $SO_4^{2-}$ (APHA, 2005). Total alkalinity was measured by titration with hydrochloric acid (APHA, 2005) using a potentiometric auto-titrator (TitraLab 865, Radiometer Analytical, Lyon, France). Concentrations of the anions $CO_3^{2-}$ and $HCO_3^{-}$ were calculated from alkalinity and pH measurements (APHA, 2005).

### 2.4. Data analysis

#### 2.4.1. Ion matrix characterization

Molar proportions of each of the eight major ions were calculated for each sample as molar concentration of each ion divided by the sum of the eight major ions. Mean molar proportions were then computed for each stream for the period Spring 2011–Spring 2013, and aggregate mean proportions were calculated by stream type.

#### 2.4.2. High-frequency specific conductance data preparation

We used HOBOWare software (Onset Computer Corp., Bourne, Massachusetts USA) to compute SC as a linear function of electrical conductivity and temperature in each study stream as recorded concurrently by the dataloggers. The dataset was then censored to exclude false SC readings observed as a result of datalogger burial by sediment or datalogger malfunction (e.g., missing data or SC ≤ 0 μS/cm). The corrected dataset was then constrained to the period 15 Oct 2011 through 14 Oct 2015. To simulate an SC sampling scheme comparable to daily grab sampling, data were further constrained to SC observed at 12:00 p.m. each day to represent daily SC.

To facilitate comparison of SC patterns among streams that span a wide range of salinity, a standardized SC metric was calculated. For each stream, we computed the SC relative deviation from mean (SCRDM) for each daily observation (SC at 12:00 p.m.):

$$SCRDM_d = \frac{SC_d - \overline{SC}}{\overline{SC}} \quad (1)$$

where $d$ = date, and $\overline{SC}$ = mean of daily SC for the four-year study period (n ≤ 1461).

We then computed the mean daily SCRDM across streams (n = 25) and years (n = 4) to yield a single SCRDM value for each day that represents deviation from long-term mean SC that is expected on a given Julian day.

#### 2.4.3. Model specification

Periodic functions can be effective for describing cyclic seasonal patterns, including those observed in water quality (DeWalle and Davies, 1997; Helsel and Hirsch, 2002; Halliday et al., 2012) and epidemiology (Stolwijk et al., 1999). Because we expected SC to vary with annual cycle of streamflow, we fit a first-harmonic sinusoidal linear model describing SCRDM as a function of Julian day:

$$SCRDM_t = \beta_0 + \beta_1 \sin\left(\frac{2\pi t}{T}\right) + \beta_2 \cos\left(\frac{2\pi t}{T}\right) + \varepsilon \quad (2)$$

where

$t$ = Julian day and $T$ = length of period in days. In this case we used a period of $T$ = 366 days because 2012 was a leap year.

We evaluated the model for error and goodness of fit and for explanatory and predictive power. In addition, we used the model to estimate SCRDM extrema and associated error, to gauge ability of the model to predict timing and magnitude of salinity extremes during the year.

Timing of minimum and maximum values of SCRDM was calculated as:

$$t_{min} = \tan^{-1}\left(\frac{\beta_1}{\beta_2}\right) \times \frac{T}{2\pi} \quad (3)$$

and

$$t_{max} = t_{min} + \frac{T}{2} \quad (4)$$

where

$t_{min}/t_{max}$ = Julian day of minimum/maximum SCRDM and T = length of period in days

The expected SCRDM value for any Julian day, $SCRDM_t$, was calculated as:

$$SCRDM_t = A \times \cos\left[\left(\frac{2\pi t}{T}\right) - \theta\right] \quad (5)$$

where

$A = \sqrt{\beta_1^2 + \beta_2^2}$, the amplitude of the sinusoidal function,
t = Julian day,
T = length of period in days (366), and
$\theta = \frac{2\pi t_{max}}{T}$, the phase shift of the cosine function in radians

#### 2.4.4. Model validation

To evaluate how the sinusoidal model might perform on novel data from other streams in the population of Appalachian headwater streams, both reference and those salinized by coal mining, we conducted model validation using a modified leave-one-out cross validation (LOOCV) procedure. Cross-validation evaluates the power of a model to predict novel independent observations in the population of interest (Arlot and Celisse, 2010), and the population of interest is that of temperate forested headwater streams. Therefore, we modified the LOOCV procedure to leave streams out of the aggregate SCRDM calculation in order to estimate model performance on a novel stream. We performed cross-validation by leaving out one of the 25 streams (test dataset) from the full dataset and conducted the same

data processing and modeling as described above on the remaining 24 streams (training dataset). We then compared predicted daily SCRDM values from the training model to observed daily SCRDM values from the test dataset to calculate cross-validation error (CVE) of the training model. We calculated CVE similarly to root mean squared error (RMSE), but instead of comparing the model predictions with data used to fit the model, model predictions are compared to observations of the single stream in the test dataset:

$$CVE_{training} = \sqrt{\frac{\sum_{t=1}^{T}\left(\widehat{SCRDM}_{t,training} - SCRDM_{t,test}\right)^2}{T}} \quad (6)$$

where $t$=Julian day and $T$=length of period in days (366). We repeated this procedure 25 times, leaving out a different stream each time, to arrive at the mean CVE (n=25).

*2.4.5. Model validation using larger-order rivers*

To test spatial scalability of the modeling approach to non-headwater streams, we fit sinusoidal models to daily SC data for five larger-order rivers (order 4 - 6) in our study region for which high-frequency SC data were available (Fig. 1). We obtained SC data from a public database of stream gages maintained by the U.S. Geological Survey (USGS). We used data from the same time period as for headwater streams (15 Oct 2011–14 Oct 2015), which yielded records of two to four years per stream. Following the same approach as for headwater streams, we selected the 12:00 p.m. value to represent a single daily sample, then relativized the raw SC to SCRDM using site-specific long-term mean SC and aggregated across sites to arrive at a single mean SCRDM value per Julian day. We fit a sinusoidal model to mean SCRDM for the larger-order rivers and computed the same model summary statistics as for the headwater-stream model. The larger-river model was evaluated for comparability to the headwater-stream model using model error, fit statistics, and extrema magnitude and timing. This analysis can be replicated by running the R script "USGS_streams.R", available in the online supplement to this article.

*2.4.6. Alternatives to high-frequency sampling*

Recognizing the challenges of daily SC measurement for practitioners who may want to characterize SC variation in streams of interest, we evaluated the feasibility of modeling annual SC using discrete sampling data gathered at longer intervals. We simulated sampling at intervals $i$=7, 14, 30, 60, and 90 days to complement the full model, which used data of $i$=1 day. For each interval, we subsampled each stream exactly every $i$ days. Because there are $i$ ways to sample every $i$ days (i.e., for $i$=7, sample all Mondays in a year, all Tuesdays in a year, etc.), for each interval we repeated the subsampling process $i$ times, shifting the subset of data by one day each time, thus yielding $i$ subsets of data. To illustrate: in the case of $i$=7, seven subsets were constructed composed of 52 days of SC observations, the first containing data for Julian days (1, 8, 15, …,358, 365) and the seventh containing data for Julian days (7, 14, 21, …,357, 364). For each interval, $i$ sub-models were constructed, one with each data subset, using the same model-fitting procedure as was used for the full model. We then performed the LOOCV procedure as above, recording the prediction error of each CV training sub-model (n=25$i$). Finally, we compared prediction errors among alternative intervals using the Games-Howell post-hoc multiple comparison test, which is robust to unequal sample sizes and heterogeneous variance among groups (Day and Quinn, 1989).

*2.4.7. Evaluation of mining influence on seasonal salinity pattern*

We modeled reference and test streams separately to determine if a seasonal SC pattern exists in the absence of mining influence. We aggregated and modeled daily SCRDM data across streams and years for test (n=20) and reference (n=5) streams as above for the full $i$=1-day model; and we compared amplitude, SCRDM extrema timing, and prediction errors to quantify differences between reference- and test-stream SC patterns.

All analyses were conducted using R (R Core Team, 2017) with test $\alpha$=0.05. All model fitting was performed using function stats::lm included with base R (R Core Team, 2017). We used userfriendlyscience::posthocTGH (Peters, 2017) for the Games-Howell multiple comparison procedure. We used the package dataRetrieval (Hirsch and De Cicco, 2015) for obtaining data on larger-order streams from the U.S. Geological Survey. The package lubridate (Grolemund and Wickham, 2011) was used for working with date values.

## 3. Results

### 3.1. Ionic composition

The dominant aqueous cation was $Ca^{2+}$ in both stream types, but $SO_4^{2-}$ was the dominant anion in salinized test streams, whereas $HCO_3^-$ was the primary anion in reference streams (Table 1). Proportions of $Mg^{2+}$ were also elevated in test streams relative to reference streams. Sodium and $Cl^-$ were not major components of salinized streams, accounting for <13% of molarity combined (Table 1).

### 3.2. Salinity pattern model

The full model identified a significant seasonal pattern of salinity, with minimum SC in spring and maximum SC in fall (Fig. 4). As expected, the model was centered on mean SC (i.e., SCRDM=0; $\beta_0$ $p>0.05$), with strong fit ($R^2$=0.82) and a narrow confidence interval of ±1.25% (Table 2). Model RMSE was approximately 7% SCRDM, and prediction error was approximately ±14% SCRDM (Table 2). Peak annual variation of salinity was approximately ±21% of mean SC (Table 3). The model predicted annual minimum SC within two weeks of the observed minimum ($T_{min}$ error=−12 days), whereas annual maximum SC was predicted almost four weeks earlier than actual ($T_{max}$ error=−25 days; Table 3).

**Table 1**
Mean mass concentrations and molar proportions of major ions by stream type, May 2011–April 2013.

| Stream Type | units | $Cl^-$ | $SO_4^{2-}$ | $CO_3^{2-}$ | $HCO_3^-$ | $Ca^{2+}$ | $K^+$ | $Mg^{2+}$ | $Na^+$ |
|---|---|---|---|---|---|---|---|---|---|
| Reference | mg/L | 2.56 | 9.65 | 0.03 | 22.94 | 6.45 | 1.30 | 2.47 | 3.40 |
| | molar proportion | 0.0834 | 0.1185 | 0.0007 | 0.3489 | 0.1655 | 0.0396 | 0.1075 | 0.1360 |
| Test | mg/L | 7.15 | 297.64 | 0.44 | 118.98 | 82.29 | 4.33 | 51.85 | 20.86 |
| | molar proportion | 0.0215 | 0.2763 | 0.0006 | 0.2060 | 0.1965 | 0.0111 | 0.1864 | 0.1016 |

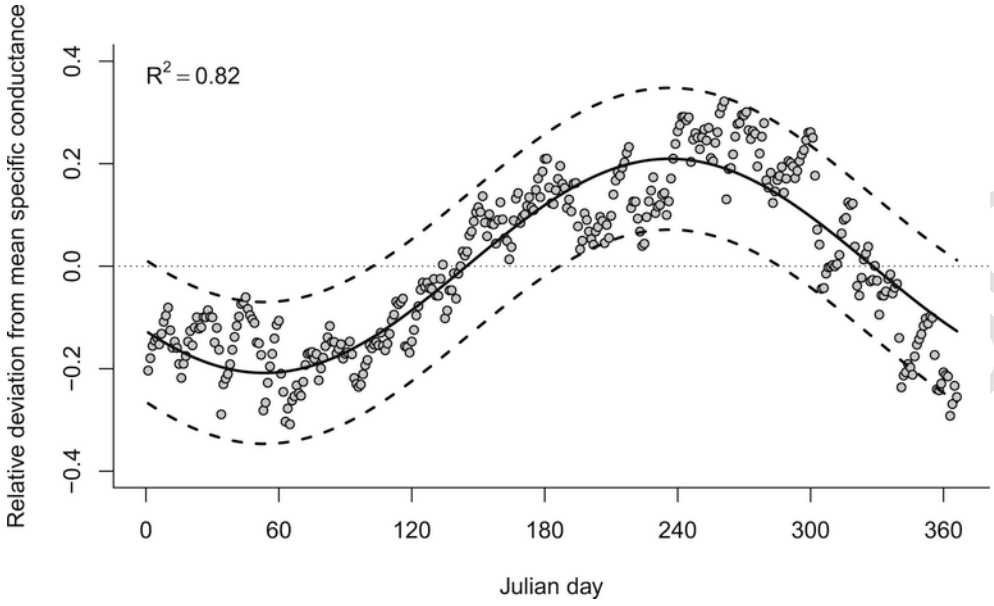


**Fig. 4.** Full model: first-harmonic sinusoidal model of relative deviation from mean specific conductance (SCRDM) by Julian day. Points are means of daily SCRDM for 25 streams during the period 15 Oct 2011–14 Oct 2015. Fitted line (solid) with 95% prediction interval (dashed).

**Table 2**
Full model summary.

| Parameter | Mean | SE | p | 95% Confidence Limits |
|---|---|---|---|---|
| $\beta_0$ (Intercept) | $6.664 \times 10^{-4}$ | $3.662 \times 10^{-3}$ | 0.8557 | $-6.535 \times 10^{-3}$, $7.867 \times 10^{-3}$ |
| $\beta_1$ (sin) | −0.1657 | $5.179 \times 10^{-3}$ | <0.0001 | −0.1759, −0.1556 |
| $\beta_2$ (cos) | −0.1272 | $5.179 \times 10^{-3}$ | <0.0001 | −0.1374, −0.1170 |
| Overall model | | | <0.0001 | |
| Adjusted $R^2$ | | 0.82 | | |
| RMSE | | 0.06986 | | |
| 95% Confidence Interval (±) | | 0.01249 | | |
| 95% Prediction Interval (±) | | 0.1385 | | |

SE: standard error of mean, RMSE: root mean square error.

**Table 3**
Full model extrema summary.

| | Estimate | Observed | Error |
|---|---|---|---|
| Extrema timing (Julian day) | | | |
| $T_{min}$ [a] | 53 | 65 | −12 |
| $T_{max}$ | 236 | 261 | −25 |
| $T_{mean}$ 1 [b] | 144 | | |
| $T_{mean}$ 2 | 328 | | |
| Extreme and mean SCRDM [c] | | | |
| at $T_{min}$ | −0.2089 | −0.2756 | 0.0667 |
| at $T_{max}$ | 0.2089 | 0.1407 | 0.0682 |
| at $T_{mean}$ 1 | 0 | 0.0246 | −0.0246 |
| at $T_{mean}$ 2 | 0 | −0.0267 | 0.0267 |
| Annual SCRDM extrema | | | |
| Minimum | −0.2089 | −0.3085 | 0.0996 |
| Maximum | 0.2089 | 0.3218 | −0.1129 |

[a] $T_{min}/T_{max}$: Julian day of minimum/maximum SCRDM.

[b] $T_{mean}1/2$: Julian day of first/second annual occurrence of mean SCRDM.

[c] SCRDM: specific conductance relative deviation from mean.

### 3.3. Model validation

The modified LOOCV procedure yielded a CVE (±SE) of 0.1384 ± 0.0119 SCRDM, indicating that the full model can be expected to estimate mean SC patterns of novel individual streams with an upper 95% confidence limit of approximately 16% SCRDM error. Mean (±SE) RMSE was lower for the full model (0.0699 ± 0.0003 SCRDM) than was observed when sinusoidal models were fit on a site-specific basis to each of the 25 streams (0.1064 ± 0.008 SCRDM). However, much of the variance in error among streams was reflected in the mean CVE of the full model (0.1384 ± 0.0116 SCRDM) (Fig. 5). This analysis revealed that individual streams can vary in their conformance to a sinusoidal pattern, but aggregation across streams creates a regional model that reveals the underlying pattern of annual periodic variation in salinity.

Validation of spatial scaling indicated that larger-order rivers exhibited seasonal patterns of SC similar to those of headwater streams. The overall model and individual sinusoidal coefficients were strongly significant ($p < 0.0001$), with overall $R^2$ of 0.80 (Fig. S1). The sinusoidal pattern had a minimum in Spring ($T_{min}$ = Julian day 59) and maximum in Fall ($T_{max}$ = Julian day 242) with an amplitude of ±0.2213 SCRDM (Table S1), values that are similar to those of the headwater-stream model (Table 2).

### 3.4. Alternatives to high-frequency sampling

Simulating alternative sampling intervals indicated a significant increase in prediction error with increasing sample interval (Fig. 6). At intervals of 7, 14, and 30 days, models reliably explained SC patterns with predictive power comparable to the 1-day model, with 95% prediction intervals increasing slightly with sampling interval, but not exceeding ±18% (Table 4). At 60 days, the mean prediction interval increased to approximately ±29%, more than twice as wide as that of the 1-day model. If sampling interval increased to 90 days, sub-models often failed to explain SC patterns (overall model $p > 0.05$) and prediction intervals were over five times wider than with the 1-day model (Table 4).

### 3.5. Evaluation of mining influence on seasonal SC pattern

Both reference and test streams exhibited significant seasonal SC patterns, with spring minima and fall maxima (Fig. 7). Reference and test models were comparable, with the reference model exhibiting an

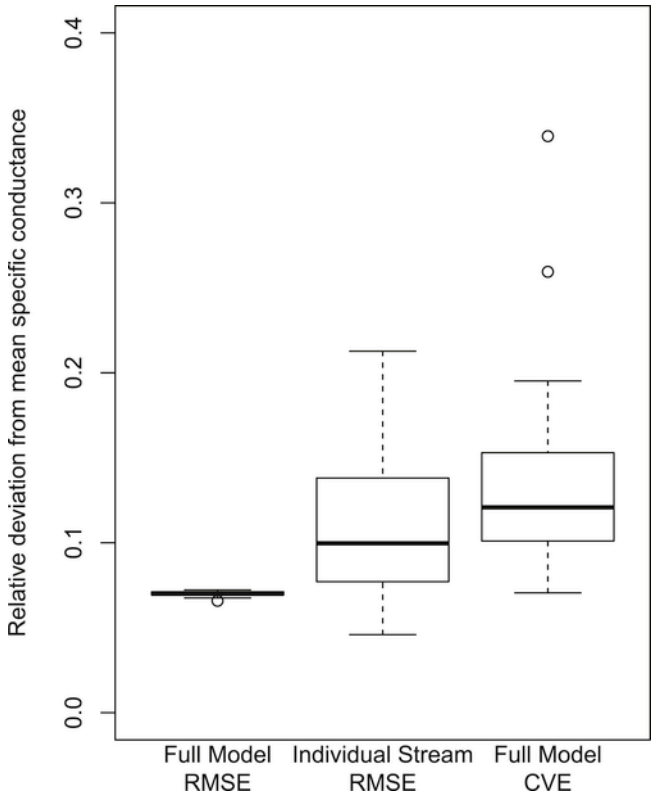


**Fig. 5.** Boxplot comparing error of aggregate and site-specific models. Full (aggregate) model root mean squared error (RMSE) is lower than RMSE for individual stream site-specific models, but much of the inter-site model error is captured in the full model cross validation error (CVE), which simulates model performance on novel streams. All models based on 1-day sampling interval, n = 25 streams.

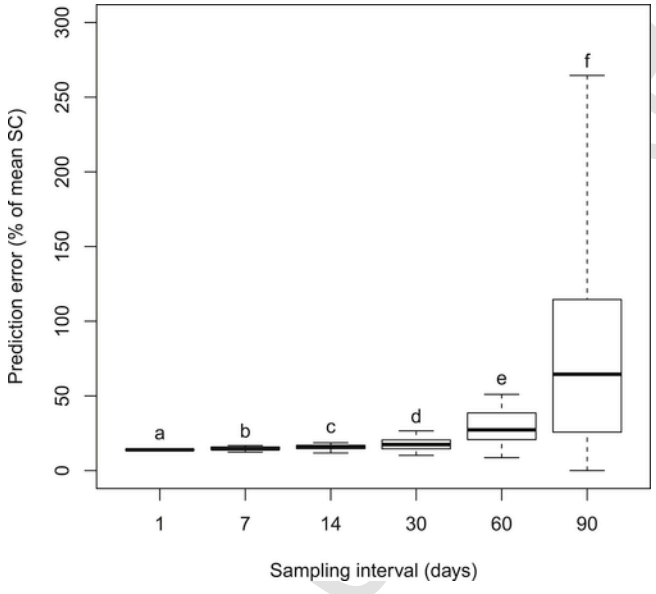


**Fig. 6.** Boxplot of prediction error for alternative sampling intervals. For each sampling interval *i*, n = 25*i*. Games-Howell multiple comparison procedure indicates significant differences ($p < 0.05$) in mean prediction error among sampling intervals with different letters.

**Table 4**
Model summary for alternative sampling intervals.

| Parameter | Sampling Interval (days) | | | | | |
|---|---|---|---|---|---|---|
| | 1 | 7 | 14 | 30 | 60 | 90 |
| Median sub-model p-values | | | | | | |
| $\beta_0$ (Intercept) | 0.8557 | 0.9465 | 0.9694 | 0.9619 | 0.9474 | 0.8648 |
| $\beta_1$ (sin) | <0.0001 | <0.0001 | <0.0001 | 0.0004 | 0.0299 | 0.0988 |
| $\beta_2$ (cos) | <0.0001 | <0.0001 | <0.0001 | 0.0031 | 0.0769 | 0.1302 |
| Overall model | <0.0001 | <0.0001 | <0.0001 | 0.0003 | 0.0392 | 0.1180 |
| Specific conductance relative deviation from mean (SCRDM) | | | | | | |
| Mean Training Model RMSE | 0.06986 | 0.07008 | 0.07081 | 0.07360 | 0.07727 | 0.09014 |
| Mean Cross-Validation Error | 0.1384 | 0.1384 | 0.1387 | 0.1398 | 0.1417 | 0.1496 |
| Mean 95% Confidence Interval (±) | 0.01249 | 0.03433 | 0.05033 | 0.07907 | 0.1685 | 0.4933 |
| Mean 95% Prediction Interval (±) | 0.1385 | 0.1470 | 0.1565 | 0.1768 | 0.2918 | 0.7534 |

RMSE: root mean squared error.

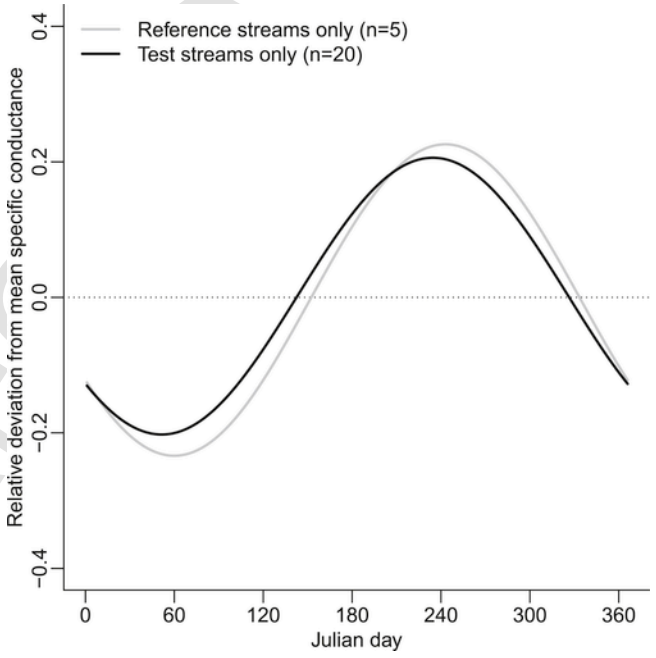


**Fig. 7.** First-harmonic sinusoidal models of relative deviation from mean specific conductance (SCRDM) by Julian day for reference and test streams separately for the period 15 Oct 2011–14 Oct 2015.

amplitude approximately 12.5% larger and later occurrence of extrema (8.5 days) as compared to the test stream model. Prediction error was also comparable between reference (±0.1350 SCRDM) and test (±0.1454 SCRDM) models. Model fit and coefficients were comparable for reference and test stream sinusoidal models, with only the sine term significantly different between models (Table 5).

## 4. Discussion

### *4.1. Drivers of the salinity pattern*

The annual pattern of salinity observed in these headwater streams appears to be the product of interactions among the geology and climate of the central Appalachian ecoregion, as well as the land-cover vegetation of the catchments studied. Geology governs the character

**Table 5**
Parameters and fit statistics for separate reference- and test-stream sinusoidal models.

| | Reference | Test |
|---|---|---|
| Adjusted $R^2$ | 0.85 | 0.79 |
| $\beta_0$ (Intercept) | −0.0039 | 0.0018 |
| SE | 0.0036 | 0.0038 |
| p | 0.2720 | 0.6390 |
| $\beta_1$ (sin) | −0.1969 | −0.1579* |
| SE | 0.0051 | 0.0054 |
| p | <0.0001 | <0.0001 |
| $\beta_2$ (cos) | −0.1184 | −0.1294 |
| SE | 0.0051 | 0.0054 |
| p | <0.0001 | <0.0001 |

*Parameter is significantly different between Reference and Test models ($p < 0.05$).

of major ions and climate influences precipitation available for weathering of geologic sources of salt. Evapotranspiration of terrestrial vegetation influences stream water yield, which in turn causes seasonal dilution or concentration of in-stream salts. In addition, respiration processes in catchment soils influence in-stream bicarbonate concentrations.

Geology influences the type of major ions that occur in freshwaters (Gibbs, 1970), and weathering by water contact dissolves and transports those ions to groundwater and surface water (Griffith, 2014). In the case of mining-influenced streams, the geologic signature is altered and amplified relative to that of unmined reference streams, causing concentrations of salts downstream of valley fills and other mining-origin influences to be elevated above background levels (Griffith et al., 2012). Geologic disturbance also influences character of the salinity produced by these watersheds where sulfate is the dominant anion, whereas bicarbonate dominates anionic composition of reference-stream water. Others have observed that Appalachian mine rocks, when freshly disturbed, produce waters with elevated proportions of sulfates relative to reference levels (Pond et al., 2008, 2014; Griffith et al., 2012; Daniels et al., 2016). Our data also show that Mg is elevated both proportionately as an ionic component and as a ratio to Ca in mining-influenced streams, relative to reference streams, a result that is consistent with other studies (Pond et al., 2008, 2014). Prior research indicates that reduced-sulfur oxidation and carbonate dissolution within the sedimentary rocks' cementing materials are among the mineral weathering reactions responsible for geologic releases (Daniels et al., 2016), but the specific mechanisms responsible for these ions' releases remain under study.

Regional climate dictates precipitation amounts and timing, which influences quantity of water available to weather and leach soluble ions from mine spoils. With relatively consistent precipitation levels throughout the year (Baily, 1995, Fig. 2), mine spoil fills located in the test-stream catchments studied here have a consistent source of water for mineral weathering and dissolution reactions that are responsible for soluble ion release. Those spoil fills discharge saline leachate that is elevated consistently over reference levels (Agouridis et al., 2012; Evans et al., 2014; Sena et al., 2014; Clark et al., 2016). Other studies have found that saline base flow is then maintained from Appalachian coal mine valley fills as a result of water storage-and-release effects of fill materials (Wiley et al., 2001; Griffith et al., 2012; Nippgen et al., 2017).

Combined geologic and climatic factors establish a relatively consistent mean salinity potential for each stream, because geologic materials influencing that character are fixed within those catchments. Baseflow SC levels of waters emerging from valley fills vary seasonally (Clark et al., 2016). However, variations in salinity are also influenced by variable dilution of saline discharge from valley fills. The sinusoidal pattern modeled here uses data that have been relativized to the mean SC, so the pattern observed describes only annual variation resultant from dilution, not absolute SC levels. Dilution is governed by seasonal changes in amount of water reaching the stream channel, which is driven by both precipitation and ET in the catchment. Stream flow is inversely proportional to ET (Croft, 1948), and increased forest cover increases ET, thus reducing stream flow during the growing season (Hibbert, 1967; Bosch and Hewlett, 1982). In this study, all streams had intact forest in the riparian zone and most stream catchments were well-forested. Overall mean forest cover was 76%, with reference streams averaging 94.3% (range: 87.4–100%) and test streams averaging 71.2% forest (range: 29.6–97.8%). Test-stream catchment forest cover 25$^{th}$ percentile was 59.5% with only three catchments having <50% forest.

If the sinusoidal shape of the annual SC pattern is influenced strongly by ET, the pattern should correspond closely with annual temperature and tree leaf phenology. Minimum SC occurs in late February to early March (Fig. 4), when deciduous trees lack leaves, catchment ET is at a minimum, and salinity dilution is at a maximum. Evapotranspiration, and in turn SC, begin to increase after leaf-out (Polgar and Primack, 2011), which occurs typically in April in the southern and central Appalachians (Lopez et al., 2008). Water yield continues to decline steadily through spring and summer (Fig. 3) as increased temperatures (Fig. 2) and growing trees with full canopy increase ET, further increasing SC, which peaks during late August to early September (Fig. 4). The observed downturn of SC during July and August may be a consequence of the above-average rainfall for July during the study period, which if delivered in the form of heavy storms would likely both infiltrate mine spoil fills, causing internal dilution, and raise peak flows in streams receiving those fill waters (Messinger and Paybins, 2003; Wiley and Brogan, 2003). Salinity begins to decline by the end of September, the point of 50% leaf fall (Lopez et al., 2008), and continues to decrease rapidly as lower temperatures and loss of leaves reduce ET, which increases streamflow.

Terrestrial vegetation may also have some influence on seasonal salinity concentration via contributions of $HCO_3^-$ produced by root respiration and other soil respiration processes, some of which likely becomes dissolved in subsurface waters and is carried to streams (Castelle and Galloway, 1990). Others have shown that such effects vary seasonally in a manner that is complementary to the seasonal pattern observed here (Jones and Mulholland, 1998). Because reference streams are less saline than test streams, the low-level $HCO_3^-$ contributions by terrestrial root respiration would be expected to have greater proportionate influence in reference streams. In contrast, test-stream $HCO_3^-$ is predominantly of geologic origin, thus minimizing the seasonal influence of root respiration on salinity in mining-influenced streams.

The case for ET, rather than precipitation, as the primary driver of the observed salinity pattern is strengthened by observation that SC extremes do not correspond to rainfall extremes. Peak monthly rainfall occurs on average in July (Fig. 2), which would be a time of maximum dilution if salinity responded primarily to rainfall. By similar reasoning, minimum dilution should occur during November, the period of minimum monthly rainfall for the study period. However, SC was greater than its annual mean during July, and had declined substantially from its annual peak by November (Fig. 4). Further, SC extrema occur at times when monthly rainfall is similar to the annual mean. Therefore, the evidence supports the conclusion that ET, through its influence on streamflow, is a primary driver of the sinusoidal pattern of salinity observed in this study. Our analysis of larger-order rivers draining the study area revealed salinity patterns

similar to those exhibited by headwater streams (Fig. S1, Table S1), demonstrating that the pattern is not confined to our study streams.

### *4.2. Evaluation of mining influence on seasonal salinity pattern*

Reference streams exhibited a strong annual cycle of SC, indicating that such a pattern is natural and not a phenomenon unique to mining-influenced streams. Although annual SC patterns were comparable between reference and test streams, there were minor, but notable, discrepancies between the two stream types. In particular, reference streams had greater amplitude of annual deviation from mean SC than did test streams, as well as later onset of annual extrema (Fig. 7). Both of these discrepancies may be attributable to differences in ET and/or base flow between stream types.

Greater amplitude of SCRDM in reference streams may be a result of greater dilution at minimum SCRDM in late winter (February–March) and lower dilution at maximum SCRDM in late summer (August–September) as compared to salinized test streams. During late winter, SCRDM was more negative for reference streams than for test streams, indicating that salinity was relatively more dilute in the former. The higher SCRDM in test streams at that time may be the result of the storage-and-release effect of mine spoil fills, which maintains relatively higher base flows in filled streams as compared to reference streams (Wiley et al., 2001; Griffith et al., 2012; Nippgen et al., 2017). If higher base flow is maintained in test streams, the dilution effect of runoff in those streams may be reduced relative to reference streams. Conversely, in late summer, salts become relatively more concentrated in reference streams than in test streams, in part because of the higher base flow in test streams, as well as reduced dilution from runoff in reference streams owing to greater forest cover and ET of the latter.

Later onset of SCRDM extrema in reference streams is likely a result of differential strength of precipitation dilution effects among stream types. In late February, as SC minimum is reached in test streams, reference streams maintain slightly higher SC levels (Fig. 7). Upon increased precipitation in March (Fig. 2) reference streams respond in the form of greater dilution of SC and thus more negative SCRDM than test streams.

Differences of SCRDM amplitude and extrema timing between stream types are slight, which suggests that reference and test streams are highly comparable. Such was the intent of this study design, to isolate salinity as the primary factor that varied among streams while keeping all other attributes as comparable as possible to reference condition. Greater differences from reference salinity patterns may be expected where catchment forest cover is substantially lower than was observed in the test-stream catchments studied here.

### *4.3. Alternatives to high-frequency sampling*

Daily measurements of SC yielded the greatest predictive power among sampling intervals, but such high-frequency data are not available or practical to collect for all streams where salinization is a concern. After evaluating model performance for several sampling scenarios, we found that sampling at least monthly increased mean model prediction error by $\leq$28% relative to sampling daily. Bimonthly and quarterly sampling increased mean prediction error by 211% and 544%, respectively. Error for 60- and 90-day models was also more variable than for models with shorter sampling intervals (Fig. 6). More critically, models based on 60- and 90-day sampling intervals were often insignificant and/or had prediction intervals that exceeded model amplitude (Table 4), which translates to an SCRDM indistinguishable from zero.

Results varied in other studies investigating optimum sampling frequency for water quality monitoring of dissolved constituents. Analysis of one year of daily samples from a surface-water monitoring network in Illinois USA found that monthly sampling was adequate for measurement of total dissolved solids, but more frequent sampling was necessary for nutrients (Harmeson and Barcelona, 1981), and that 30-day intervals were adequate for describing seasonal variation for a suite of five parameters that included total dissolved solids (Loftis and Ward, 1980). In South Korea, analysis of high-frequency water quality data from small streams draining mountainous forested watersheds indicated that weekly to monthly sampling was adequate for characterizing seasonal patterns of solutes (Lee et al., 2015).

### *4.4. Transferability of salinity model*

The exact model defined here is not broadly transferrable as-is because specifics of salinity patterns observed in this study are influenced by regional geology, climate, and catchment land cover, as discussed above. However, because the sinusoidal pattern fundamentally describes seasonal dilution effects, the model framework may be adaptable to other streams in which salinity responds to seasonal patterns of dilution. Such a water cycle would be expected in other temperate forests of the world, but models may also be developed for streams in arid regions where precipitation patterns, rather than ET, drive dilution of salinity. We demonstrated that the seasonal pattern has similar timing and amplitude in larger-order rivers in the region, suggesting that the modeling approach should scale well spatially. Incorporating precipitation and/or stream discharge into the model could improve broad-scale model performance. Seasonal, inverse relationships between stream flow and salinity appear common in systems where chronic non-point sources of salt create chronically elevated salinity, as have been observed in Spain (Olıas et al., 2004), Canada (Bhangu and Whitfield, 1997), and Uzbekistan (Crosa et al., 2006). However, such predictable salinity-streamflow relationships are unlikely in salinized streams that do not have chronic salt stress, or where salinity does not vary with natural water cycles. For example, the sinusoidal model may not be appropriate in streams with managed mining discharge, sporadic pulsed inputs from road de-icing salts, agricultural runoff, or industrial point-sources.

## 5. Conclusions

As salinization increasingly threatens integrity of freshwaters globally, tools for describing and estimating patterns of major ion concentration in lotic systems will likely become increasingly critical for water resource managers seeking to mitigate salinization effects. High-frequency monitoring can reveal the annual pattern of salinity, while also providing the detail necessary to infer mechanisms influencing such variation. Despite anthropogenic influence, intra-annual variation of salinity in temperate forested headwater streams of central Appalachia follows a natural pattern, driven by interactive influences of climate, geology, and terrestrial vegetation on water quantity and quality. Because climatic and vegetation dynamics vary annually in a seasonal, cyclic manner, a sinusoidal periodic function can be used to fit a model to the salinity pattern. In lieu of high-frequency data, discrete samples collected at longer intervals may be adequate to characterize annual salinity patterns, but model prediction error increases rapidly as sampling interval exceeds 30 days. The modeling approach is adaptable to other systems with streamflow-dependent chronic salinity stress, and can be scaled spatially and temporally to account for site-specific factors or climatic trends.

## Acknowledgements

This work was funded jointly by the U.S. Office of Surface Mining Reclamation and Enforcement, and the Virginia Department of Mines Minerals and Energy under Cooperative Agreement number S12AC20023. We thank the many landowners, mine operators, and agency personnel who facilitated site selection and access. We also thank two anonymous reviewers for their helpful suggestions.

## Appendix A. Supplementary data

Supplementary data related to this article can be found at https://doi.org/10.1016/j.watres.2018.01.012.

## References

Agouridis, C.T., Angel, P.N., Taylor, T.J., Barton, C.D., Warner, R.C., Yu, X., Wood, C., 2012. Water quality characteristics of discharge from reforested loose-dumped mine spoil in eastern Kentucky. J. Environ. Qual. 41 (2), 454–468.

APHA, 2005. Standard Methods for the Examination of Water and Wastewater, twenty-first ed. American Public Health Association, Washington, DC, 1220pp.

Arlot, S., Celisse, A., 2010. A survey of cross-validation procedures for model selection. Stat. Surv. 4, 40–79. https://doi.org/10.1214/09-SS054 http://projecteuclid.org/euclid.ssu/1268143839.

Baily, R.G., 1995. Description of the Ecoregions of the United States, second ed. USDA Forest Service, Washington, DC, https://doi.org/10.1080/04597229308460051.

Bernhardt, E.S., Lutz, B.D., King, R.S., et al., 2012. How many mountains can we mine? Assessing the regional degradation of central Appalachian rivers by surface coal mining. Environ. Sci. Technol. 46, 8115–8122. https://doi.org/10.1021/es301144q.

Bhangu, I., Whitfield, P.H., 1997. Seasonal and long-term variations in water quality of the skeena river at usk, british Columbia. Water Res. 31 (9), 2187–2194.

Bosch, J.M., Hewlett, J.D., 1982. A review of catchment experiments to determine the effect of vegetation changes on water yield and evapotranspiration. J. Hydrol. 55, 3–23.

Cañedo-Argüelles, M., Hawkins, C.P., Kefford, B.J., et al., 2016. Saving freshwater from salts. Science 351, 914–916. https://doi.org/10.1126/science.aad3488.

Cañedo-Argüelles, M., Kefford, B.J., Piscart, C., et al., 2013. Salinisation of rivers: an urgent ecological issue. Environ. Pollut. 173, 157–167.

Castelle, A.J., Galloway, J.N., 1990. Carbon dioxide dynamics in acid forest soils in shenandoah national park, Virginia. Soil Sci. Soc. Am. J. 54, 252–257.

Clark, E.V., Greer, B.M., Zipper, C.E., Hester, E.T., 2016. Specific conductance–stage relationships in Appalachian valley fill streams. Environ. Earth Sci. 75 (17), 1222.

Cormier, S.M., Suter, G.W., 2013. A method for deriving water-quality benchmarks using field data. Environ. Toxicol. Chem. 32, 255–262. https://doi.org/10.1002/etc.2057.

Croft, A.R., 1948. Water loss by stream surface evaporation and transpiration by riparian vegetation. Eos Trans. Am. Geophys. Union 29, 235–239. https://doi.org/10.1029/TR029i002p00235.

Crosa, G., Froebrich, J., Nikolayenko, V., Stefani, F., Galli, P., Calamari, D., 2006. Spatial and seasonal variations in the water quality of the amu darya river (central asia). Water Res. 40 (11), 2237–2245.

Daniels, W.L., et al., 2016. Predicting total dissolved solids release from central Appalachian coal mine spoils. Environ. Pollut. 216, 371–379. https://doi.org/10.1016/j.envpol.2016.05.044.

Day, R., Quinn, G., 1989. Comparisons of treatments after an analysis of variance in ecology. Ecol. Monogr. 59 (4), 433–463. https://doi.org/10.2307/1943075.

DeWalle, D.R., Davies, T.D., 1997. Seasonal variations in acid-neutralizing capacity in 13 northeast United States headwater streams. Water Resour. Res. 33, 801–807. https://doi.org/10.1029/96WR03852.

Evans, D.M., Zipper, C.E., Donovan, P.F., Daniels, W.L., 2014. Long-term trends of specific conductance in waters discharged by Coal-mine valley fills in central Appalachia, USA. J. Am. Water Resour. Assoc. 50, 1449–1460. https://doi.org/10.1111/jawr.12198.

Gibbs, J.R., 1970. Mechanisms controlling world water chemistry. Science 170, 1088–1090. https://doi.org/10.1126/science.170.3962.1088.

Goetsch, P.A., Palmer, C.G., 1997. Salinity tolerances of selected macroinvertebrates of the sabie river, kruger national park, South Africa. Arch. Environ. Contam. Toxicol. 32, 32–41. https://doi.org/10.1007/s002449900152.

Griffith, M.B., Norton, S.B., Alexander, L.C., et al., 2012. The effects of mountaintop mines and valley fills on the physicochemical quality of stream ecosystems in the central Appalachians: a review. Sci. Total Environ. 417–418, 1–12. https://doi.org/10.1016/j.scitotenv.2011.12.042.

Griffith, M.B., 2014. Natural variation and current reference for specific conductivity and major ions in wadeable streams of the conterminous USA. Freshw. Sci. 33, 1–17. https://doi.org/10.1086/674704.

Grolemund, G., Wickham, H., 2011. Dates and times made easy with lubridate. J. Stat. Software 40 (3), 1–25 http://www.jstatsoft.org/v40/i03/.

Halliday, S.J., Wade, A.J., Skeffington, R.A., Neal, C., Reynolds, B., Rowland, P., Neal, M., Norris, D., 2012. An analysis of long-term trends, seasonality and short-term dynamics in water quality data from Plynlimon. Wales. Sci. Total Environ 434, 186–200. https://doi.org/10.1016/j.scitotenv.2011.10.052.

Hancock, G.R., Wright, A., De Silva, H., 2005. Long-term final void salinity prediction for a post-mining landscape in the Hunter Valley, New South Wales, Australia. Hydrol. Process. 19, 387–401. https://doi.org/10.1002/hyp.5538.

Harmeson, R.H., Barcelona, M.J., 1981. Sampling Frequency for Water Quality Monitoring. Illinois State Water Survey.

Helsel, D.R., Hirsch, R.M., 2002. Statistical Methods in Water Resources. U.S. Geological Survey, 522 pp.

Hem, D., 1985. Study and Interpretation of the Chemical Characteristics of Natural Water, third ed. U.S. Geological Survey, Alexandria, Virginia, 263 pp.

Hibbert, A.R., 1967. Forest treatment effects on water yield. In: Sopper, W.E., Lull, H.W. (Eds.), Int. Symp. for. Hydrol. Pergamon, Oxford, 813 pp.

Hirsch, R.M., De Cicco, L.A., 2015. User Guide to Exploration and Graphics for RivEr Trends (EGRET) and DataRetrieval: R Packages for Hydrologic Data (Version 2.0, February 2015), U.S. Geological Survey Techniques and Methods book 4, chap. A10, 93 pp. https://doi.org/10.3133/tm4A10.

Jones Jr., J.B., Mulholland, P.J., 1998. Carbon dioxide variation in a hardwood forest stream: an integrative measure of whole catchment soil respiration. Ecosystems 1, 183–196.

Lee, H.J., Chun, K.W., Shope, C.L., Park, J.H., 2015. Multiple time-scale monitoring to address dynamic seasonality and storm pulses of stream water quality in mountainous watersheds. Water 7 (11), 6117–6138.

Li, J., Zipper, C.E., Donovan, P.F., Wynne, R.H., Oliphant, A.J., 2015. Reconstructing disturbance history for an intensively mined region by time-series analysis of Landsat imagery. Environ. Monit. Assess. 187 (9), 557.

Likens, G.E., Bormann, F.H., 1995. Biogeochemistry in a Forested Ecosystem, second ed. Springer-Verlag, New York, 159 pp.

Loftis, J.C., Ward, R.C., 1980. Water quality monitoring—some practical sampling frequency considerations. Environ. Manag. 4 (6), 521–526.

Lopez, O.R., Farris-Lopez, K., Montgomery, R.A., Givnish, T.J., 2008. Leaf phenology in relation to canopy closure in southern Appalachian trees. Am. J. Bot. 95 (11), 1395–1407.

Messinger, T., Paybins, K.S., 2003. Relations between Precipitation and Daily and Monthly Mean Flows in Gaged, Unmined and Valley-filled Watersheds, Ballard Fork, West Virginia, 1999-2001. US Department of the Interior, (US Geological Survey).

Millennium Ecosystem Assessment, 2005. Ecosystems and Human Well-being: Synthesis. Island Press, Washington, DC, 137 pp.

MRLC, 2017. National land cover database. Multi-Resolution Land Characteristics consortium http://www.mrlc.gov/.

Nippgen, F., Ross, M.R., Bernhardt, E.S., McGlynn, B.L., 2017. Creating a more perennial Problem? Mountaintop removal coal mining enhances and sustains saline baseflows of appalachian watersheds. Environ. Sci. Technol. https://doi.org/10.1021/acs.est.7b02288.

Olias, M., Nieto, J.M., Sarmiento, A.M., Cerón, J.C., Cánovas, C.R., 2004. Seasonal water quality variations in a river affected by acid mine drainage: the Odiel River (South West Spain). Sci. Total Environ. 333 (1), 267–281.

Omernik, J.M., 1987. Ecoregions of the conterminous United States. Ann. Assoc. Am. Geogr. 77, 118–125.

Omernik, J.M., Griffith, G.E., 2014. Ecoregions of the conterminous United States: evolution of a hierarchical spatial framework. Environ. Manage 54, 1249–1266. https://doi.org/10.1007/s00267-014-0364-1.

Peters, G., 2017. Userfriendlyscience: Quantitative Analysis Made Accessible. R Package Version 0.6-0. http://userfriendlyscience.com.

Polgar, C.A., Primack, R.B., 2011. Leaf-out phenology of temperate woody plants: from trees to ecosystems. New Phytol. 191 (4), 926–941.

Pond, G.J., Passmore, M.E., Borsuk, F.A., et al., 2008. Downstream effects of mountaintop coal mining: comparing biological conditions using family- and genus-level macroinvertebrate bioassessment tools. J. North Am. Benthol. Soc. 27, 717–737. https://doi.org/10.1899/08-015.1.

Pond, G.J., 2010. Patterns of Ephemeroptera taxa loss in Appalachian headwater streams (Kentucky, USA). Hydrobiologia 641 (1), 185–201.

Pond, G.J., 2012. Biodiversity loss in Appalachian headwater streams (Kentucky, USA): Plecoptera and Trichoptera communities. Hydrobiologia 679 (1), 97–117.

Pond, G.J., Passmore, M.E., Pointon, N.D., et al., 2014. Long-term impacts on macroinvertebrates downstream of reclaimed mountaintop mining valley fills in central Appalachia. Environ. Manage 54, 919–933. https://doi.org/10.1007/s00267-014-0319-6.

R Core Team, 2017. R: a Language and Environment for Statistical Computing. R Foundation for Statistical Computing, Vienna, Austria http://www.R-project.org/.

Schreck, P., 1995. Environmental impact of uncontrolled waste disposal in mining and industrial areas in Central Germany. Environ. Geol. 35, 66–72.

Sena, K., et al., 2014. Influence of spoil type on chemistry and hydrology of interflow on a surface coal mine in the eastern us coalfield. Water Air Soil Pollut. 225 (11)https://doi.org/10.1007/s11270-014-2171-y.

Stolwijk, A.M., Straatman, H., Zielhuis, G.A., 1999. Studying seasonality by using sine and cosine functions in regression analysis. J. Epidemiol. Community Health 53 (4), 235–238.

Timpano, A.J., Schoenholtz, S.H., Soucek, D.J., Zipper, C.E., 2015. Salinity as a limiting factor for biological condition in mining-influenced Central Appalachian headwater streams. J. Am. Water Resour. Assoc. 51 (1), 240–250. https://doi.org/10.1111/jawr.12247.

USEPA, 2012. National Hydrography Dataset Plus – NHDPlus. Version 2.10. U.S. Environmental Protection Agency.

USNOAA, 2017. Climate Data Online. U.S. National Oceanic and Atmospheric Administration, Data retrieved 11 July 2017 http://www.ncdc.noaa.gov/cdo-web/.

Wiley, J.B., Brogan, F.D., 2003. Comparison of Peak Discharges Among Sites with and without Valley Fills for the July 8-9, 2001 Flood in the Headwaters of Clear Fork, Coal River Basin, Mountaintop Coal-mining Region, Southern West Virginia (No. 2003-133).

Wiley, J.B., Evaldi, R.D., Eychaner, J.H., Chambers, D.B., 2001. Water Resources Investigations Report Reconnaissance of Stream Geomorphology, Low Streamflow, and Stream Temperature in the Mountaintop Coal-mining Region, Southern West Virginia, 1999-2000, vol. 4092, United States Geological Survey, 42.

Williams, W.D., 1987. Salinization of rivers and streams–an important environmental hazard. Ambio 16, 180–185.

Williams, W.D., 2001. Arthropogenic salinisation of inland waters. Hydrobiologia 466, 329–337. https://doi.org/10.1007/978-94-017-2934-5_30.